Case Study of Liquefaction Mitigation by Compaction Grouting

Fred Yi
Mid Pacific Engineering Inc, Colton, USA, info@GeoAdvanced.com

Robert J. Johnson
Robert Johnson-Geotechnical Consultant/Riverside, USA, bobjgeo@yahoo.com

ABSTRACT: Ground improvement is one method used for liquefaction mitigation. Various ground improvement techniques, such as vibro-compaction, vibro-replacement stone columns and grouting are used in construction to mitigate liquefaction. Varying methods of mitigation have different advantages and limitations. In this paper, the effectiveness of liquefaction mitigation using compaction grouting is evaluated by the comparison of pre- and post-grouting cone penetration testing (CPT) results. Detailed discussions of the factors affecting the evaluation of post-grouting performance of the compaction grout method are made. In the comparison of pre- and post-grout CPT data, a *pseudo-sandification* phenomenon was noticed. A correction method for this *pseudo-sandification* phenomenon is proposed. Future research needs and improvements used for liquefaction mitigation using compaction grouting are also discussed.

Keywords: liquefaction mitigation; ground improvement; compaction grouting; cone penetration test, pseudo-sandification

1. Introduction

The destruction caused by liquefaction has been widely observed and documented after various earthquakes. Because of the tremendous damage to above-ground structures and underground lifelines caused by liquefaction-induced settlement and/or lateral spreading, a successful mitigation of liquefaction potential of a liquefiable project site is fundamental to minimizing property damage and life and safety issues.

In this paper, the performance of compaction grouting (CG), in terms of mitigating liquefaction-induced settlement, is evaluated based on the comparison of pre- and post-grouting cone penetration testing (CPT) results. Methods of site evaluation and the factors affecting the evaluation of CG performance are discussed. In the comparison of pre- and post-grout CPT data, the authors noted that the Soil Behavior Type (SBT) Index (I_c) decreased post grouting, which resulted in the SBT Index changing from silty type condition to sandy type condition. The authors call this change a *pseudo-sandification* phenomenon. A correction for the *pseudo-sandification* phenomenon is proposed. Future research needs and improvements for liquefaction mitigation using compaction grouting are also discussed.

2. Site geology and subsurface soil conditions

2.1. Site geology

The project site is located in the San Bernardino Valley, a structural basin of the northern Peninsular Ranges geomorphic province. The valley is bordered to the north and east by the northwest-to-southeast trending San Andreas fault zone and the San Bernardino Mountains. The San Jacinto fault zone, located southwest of the site, forms the boundary between two low-relief regions; the Perris Block and the San Jacinto Mountains Block (Morton and Miller [1]). The site is approximately 420 meters northeast of the Loma Linda fault, a branch of the San Jacinto fault zone.

The San Bernardino Valley itself is formed by a structurally down-dropped block of crystalline bedrock overlain by a thick accumulation of alluvium composed of floodplain and alluvial-fan deposits derived from highlands located to the south, east, north and northwest.

2.2. Subsurface soil conditions

The native geologic materials beneath the studied site consist of young alluvial-fan deposits of Holocene age. The site exploration data indicates that the project site is capped with approximately 1.5 to 2.4 meters of fill material classified as silty sand. The native soils consist of very loose to loose silty sand and sand with interbedded silt layers varying in thickness between 6.1 and 9.8 meters, underlain by medium dense to dense sand with silt, silty sand, and sandy silt layers to a depth of approximately 22 meters below the existing ground surface. Fig. 1 shows the soil profiles obtained from two exploratory borings. Also noteworthy is that the silty sand layers contain relatively high fines content (FC), shown as SM-ML in Fig. 1. The fines content range between 42% and 46% at depths above 7.6 meters and between 35% and 49% at depths below 12.2 meters.

2.3. Design groundwater depth

Groundwater was not encountered in the field exploration to the depth explored of approximately 22 meters below the existing ground surface. However, the site is mapped as within a liquefiable zone in the City's General Plan. There is also a water pond immediately east of the site. As such, the project design groundwater depth was set as 3 meters below the existing ground surface based

on the historical high groundwater data by the geotechnical firm that performed initial site investigation.

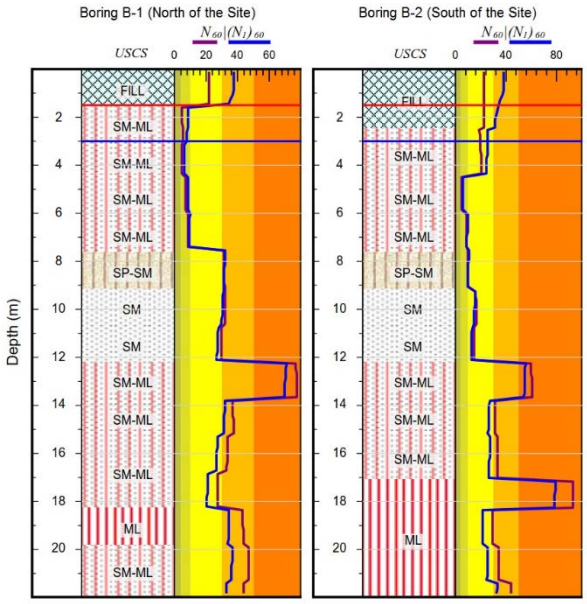

Figure 1. Soil Profiles from Exploratory Borings

2.4. Design ground motion

Per the 2010 California Building Code, the project was to be designed for a Maximum Considered Earthquake (MCE). The site-specific design spectra analysis indicates an MCE Peak Ground Acceleration (PGA_M) of 0.74 g. A Maximum Moment Magnitude (M) of 7.0 was to be used in the design.

2.5. Anticipated seismic settlement

The liquefaction potential and liquefaction-induced settlement of the site were evaluated for the soil profiles generated from Borings B-1 and B-2 (see Fig. 1) using the simplified procedure described by Idriss and Boulanger [2, 3, 4]. The computer program, GeoSuite© [7], developed by the first author, was used for the calculations. Results obtained using conventional fines contents correction [5, 6] indicate a potential liquefaction-induced settlement of between 19.8 and 28.9 centimeters (Fig. 2).

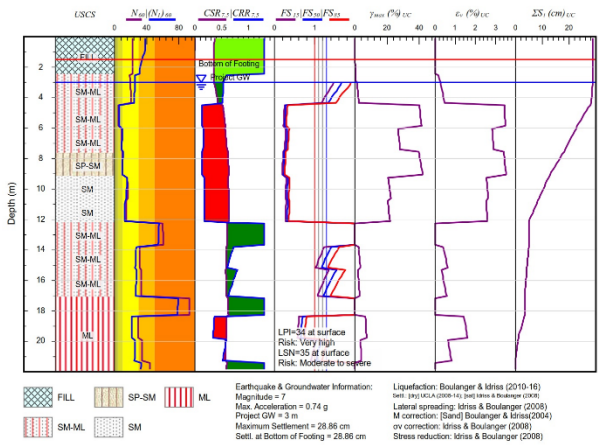

Figure 2. Sample of Liquefaction Potential and Seismic Settlement of the Existing Ground

3. Ground improvement program

3.1. Ground improvement plan

The calculated liquefaction-induced settlement is much greater than the specified maximum allowable settlement of 2.5 centimeters. In order to mitigate the liquefaction-induced settlement to satisfy the project design requirements, the CG method was proposed and accepted by the owner as the remediation method of choice.

The grouting contractor proposed a ground improvement plan with the CG column grid spacing of 2.1 meters (7 feet) on-center, each way, as shown in Fig. 3. The targeted grouting depth proposed was between 3 and 12 meters with vertical stage intervals of 1-meter. The grout was injected at each stage depth until one of the following criteria was satisfied:

1. Predetermined Replacement Ratio (R_r)
2. Grouting header pressure of 2.76 megapascal
3. Ground surface heave of 6.35 milimeter (1/4")

The R_r is defined by Eq. (1):

$$R_r = \frac{CG\ Volume}{Treatment\ Volume}\ (\%) \qquad (1)$$

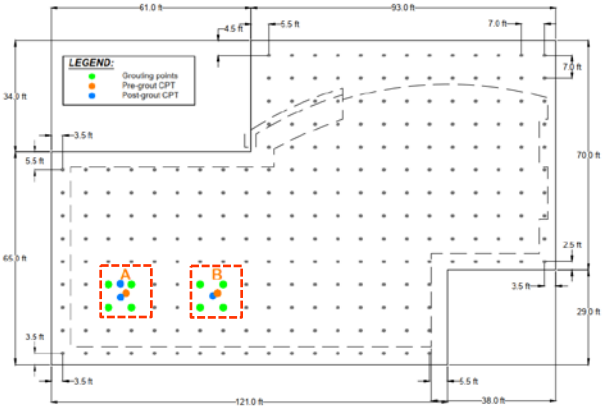

Figure 3. Ground Improvement Plan

Fig. 4 shows the grout pump utilized. The pertinent specifications of this pump are as follow:

- Maximum theoretical output: 13.8 m^3/hour
- Maximum pressure: 115 Bar
- Maximum rated strokes/minute: 30/Min.

Figure 4. Reed B20 Grout Pump

3.2. Performance verification program

In order to verify the performance of the CG method, a test program was developed prior to commencing the process over the entire site. The test program consisted of selecting two areas, test Grid A and test Grid B (see Fig. 3) and grouting the four corners of each test area. The performance of CG was assessed by CPT soundings. One CPT sounding was performed in each test grid. Grout injections were then performed at the four corner points of Grid A using a R_r of 20% and at the four corner points of Grid B using a R_r of 10%. Upon completion of grouting, post-grouting CPT soundings were performed. Fig. 5 shows a close up of the layout of test Grids A and B and the pre- and post-grout CPT points.

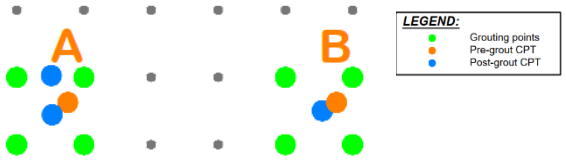

Figure 5. Test Grids and Pre- and Post-Grout CPT Points

The comparison of the tip resistance of pre- and post-grout CPT is shown in Fig. 6. It is clear that for R_r of 10%, there is generally no significant increase of tip resistance below the depth of approximately 4 meters although significant increase was observed between depths of 3 and 4 meters. For R_r of 20%, the average increase of tip resistance below depth of 3 meters is 240% to 260% for post-grout CPT-1A and CPT-1B (both excluding the extreme high values), respectively.

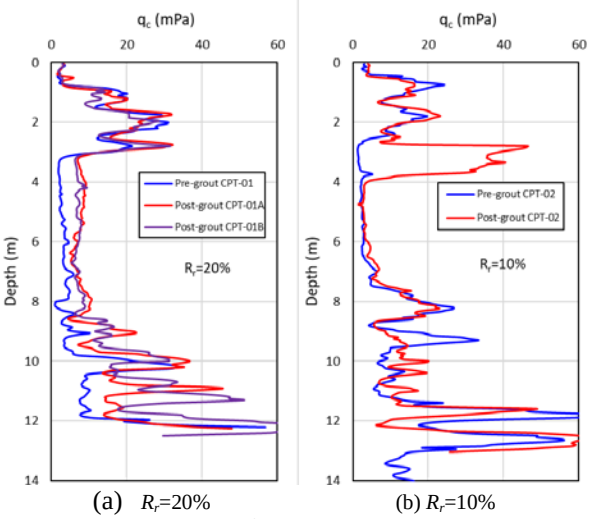

(a) R_r=20% (b) R_r=10%

Figure 6. Comparison of Tip Resistance, Pre- and Post-Grout

4. Evaluation of post-grouting performance

The performance of the grouting method was quantified in terms of liquefaction-induced settlement calculated using simplified procedures [8, 9, 10]. Using the simplified procedures, the liquefaction-induced settlement in a free-field is usually calculated using the following steps:

a) Calculate cyclic shear stress ratio.
b) Calculate cyclic shear resistance ratio.
c) Calculate liquefaction potential in terms of factor of safety against liquefaction.
d) Calculate liquefaction-induced maximum shear strain.
e) Calculate liquefaction-induced volumetric strain.
f) Integrate the volumetric strain to calculate liquefaction-induced settlement.

The existence of CG columns changes the responses of the soils between the grout columns during earthquake shaking. Also, the post-grout CPT data is changed because of the densification effects. In order to appropriately evaluate the post-grouting behavior, these effects have to be considered. The change in the response and the data results in the need for a correction factor that will be applied. The following sections will summarize the above-mentioned procedures and corresponding corrections.

4.1. Liquefaction potential

Liquefaction potential is quantified as the factor of safety against liquefaction, with liquefaction being defined as the ratio of cyclic resistance ratio (CRR_M) that will cause liquefaction of the soil to the cyclic stress ratio (CSR) developed in the soil by the earthquake.

$$FS_{liq} = CRR_{M,\sigma'_v}/CSR \quad (2)$$

4.1.1. Cyclic stress ratio (CSR)

In the simplified procedure, the CSR developed in the soil is calculated from a formula that incorporates ground surface acceleration, total and effective stresses in the soil at different depths (which in turn are related to the location of the groundwater table), non-rigidity of the soil column, and a number of simplifying assumptions. Seed and Idriss et al. [8] formulated the following equation for calculation of CSR:

$$CSR = \tau_{av}/\sigma'_{v0} = 0.65(a_{max}/g)(\sigma_{v0}/\sigma'_{v0})r_d \quad (3)$$

where τ_{av} is the average equivalent uniform cyclic shear stress caused by the earthquake and is assumed to be 0.65 of the maximum induced stress; a_{max} is the peak horizontal acceleration at ground surface generated by the earthquake; g is the acceleration of gravity; σ_{v0} and σ'_{v0} are the total and effective overburden stresses, respectively, and r_d is a stress reduction coefficient [11, 12].

4.1.2. Cyclic resistance ratio (CRR)

Various correlations between CRR and CPT tip resistance were proposed [2, 3, 4, 13, 14]. A modified version [14] of Robertson and Wride's [13] equation is as shown below:

$$CRR_{7.5} = 93 \cdot \left[\frac{Q_{tn,cs}}{1000}\right]^3 + 0.08, if\ 50 \le Q_{tn,cs} < 160$$
$$CRR_{7.5} = 0.833 \cdot \left[\frac{Q_{tn,cs}}{1000}\right] + 0.05, if\ Q_{tn,cs} < 50 \quad (4)$$

where $Q_{tn,cs} = K_c Q_{tn}$ and

$$Q_{tn} = [(q_t - \sigma_v)/p_a](p_a/\sigma'_{v0})^n \quad (5)$$

Robertson [15] updated the stress normalization by Zhang et al. [16] to allow for a variation of the stress

exponent with both normalized Soil Behavior Type (SBT_n) Index (I_c) and effective overburden stress using:

$$n = 0.381(I_c) + 0.05(\sigma'_{v0}/p_a) - 0.15 \quad (6)$$

K_c is a function of I_c and

$$I_c = [(3.47 - logQ_{t1})^2 + (logF_r + 1.22)^2]^{0.5} \quad (7)$$

where $Q_{t1} = (q_t - \sigma_{v0})/\sigma'_{v0}$ and $F_r = [f_s/(q_t - \sigma_{v0})] \cdot 100\%$.

The most recent deterministic CPT-based clean sand equivalent correlation proposed by Boulanger and Idriss [3, 4] is as follows:

$$CRR_{M=7.5,\sigma'_v=1\ atm} = Exp\left(\frac{q_{c1Ncs}}{113} + \left(\frac{q_{c1Ncs}}{1000}\right)^2 - \left(\frac{q_{c1Ncs}}{140}\right)^3 + \left(\frac{q_{c1Ncs}}{137}\right)^4 - 2.8\right) \quad (8)$$

where $CRR_{M=7.5,\sigma'_v=1\ atm}$ is the CRR at M=7.5 and σ'_v = 1 atm.

Research indicates that other corrections, such as earthquake magnitude, overburden pressure, and static shear stress, should also be made to the CRR:

$$CRR_{M,\sigma'_v} = CRR_{M=7.5,\sigma'_v=1\ atm} \cdot MFS \cdot K_\sigma \quad (9)$$

where *MSF* is earthquake magnitude scaling factor and K_σ is the overburden correction factor.

4.1.3. Maximum shear strain, γ_{max}

In the process of estimating liquefaction-induced settlement, Ishihara and Yoshimine [17] discovered that for a given value of initial relative density (D_R) of soil, the smaller the factor of safety, the larger the maximum shear strain, γ_{max}, while at a given value of FS_{liq} less than unity, the larger the D_R, the smaller the γ_{max}. A set of relationships between FS_{liq} and γ_{max} was established for given values of D_R. Yoshimine et al [18] approximated these relationships with a hyperbolic function as expressed in Eqs. (10) and (11).

$$\gamma_{max} = 0, if\ FS_{liq} \geq 2 \quad (10a)$$

$$\gamma_{max} = 0.035(2 - FS_{liq})\left(\frac{1-F_\alpha}{FS_{liq}-F_\alpha}\right), if\ 2 > FS_{liq} \geq F_\alpha \quad (10b)$$

$$\gamma_{max} = \infty, if\ FS_{liq} < F_\alpha \quad (10c)$$

$$F_\alpha = 0.032 + 4.7D_R - 6.0(D_R)^2 \quad (11)$$

For CPT data, Idriss and Boulanger [2] derived an expression as:

$$F_\alpha = -11.74 + 8.34(q_{c1Ncs})^{0.264} - 1.371(q_{c1Ncs})^{0.528} \quad (12)$$

with q_{c1Ncs} limited to values ≥ 69 for use in this expression.

4.1.4. Post-liquefaction volumetric strain, ε_v

Ishihara and Yoshimine [17] observed that the ε_v of clean sand that occurs during post-liquefaction reconsolidation was directly related to the γ_{max} developed during undrained cyclic loading and to the initial D_R.:

$$\varepsilon_v = 1.5 \cdot exp(-2.5D_R) \cdot min(0.08, \gamma_{max}) \quad (13)$$

According to Idriss and Boulanger [2], this equation can be expressed in terms of CPT penetration resistances as follows:

$$\varepsilon_v = 1.5 \cdot exp(2.551 - 1.147(q_{c1Ncs})^{0.264}) \cdot min(0.08, \gamma_{max}) \quad (14)$$

4.1.5. Liquefaction-induced settlement

Idriss and Boulanger [2] indicates that the ground surface settlement for one-dimensional reconsolidation can be computed by equating the vertical strains to the volumetric strains (as is appropriate for one-dimensional reconsolidation) and then integrating the vertical strains over the depth interval of concern:

$$S_{v,1D} = \int_0^{Z_{max}} \varepsilon_v \cdot dz \quad (15)$$

4.2. Shear stress reduction caused by CG columns

In current design practice, it is common that the seismic shear stress of the soils among discrete columns, such as stone and soil-cement columns, will be reduced due to the existence of these columns, that is:

$$(\tau_{av})_{sc} = \tau_{av} \cdot K_G \quad (16)$$

where τ_{av} and $(\tau_{av})_{sc}$ are seismic shear stress in soils before and after improvement respectively, and K_G is defined as the shear-stress reduction factor.

$$K_G = \frac{(\tau_{av})_{sc}}{\tau_{av}} = \frac{CSR_I}{CSR} \quad (17)$$

where CSR_I is cyclic stress ratio with ground improvement.

The shear-stress reduction factor concept was originally introduced by Baez [19] and Baez and Martin [20] for evaluating the reduction of soil liquefaction by vibro-stone columns. Baez and Martin [20] derived the following equation by assuming the shear strain compatibility, i.e., the shear strains for both loose (soil) and stiff (column) materials are compactible.

$$K_G = \frac{1}{[G_r \cdot A_r + (1 - A_r)]} \quad (18)$$

where A_r is the area replacement ratio ($A_r = A_{sc}/A$); G_r is the shear-modulus ratio ($G_r = G_{sc}/G_s$); A_{sc} is the area of the stone column; A is total plan area (sum of area of soil and stone column); G_{sc} is the shear modulus of the stone column; and G_s is the shear modulus of soil. Baez and Martin [20] reported G_r values between 2 and 7 for stone columns, whereas larger values can be expected for soil-cement columns.

Generally, $R_r = A_r$.

Rayamajhi et al. [21, 22, 23, 24] reported that Eq. (18) significantly overestimates the reduction in seismic shear stresses and proposed a modification as shown in Eq. (19).

$$K_G = \frac{1}{[G_r \cdot A_r \cdot \gamma_r + (1 - A_r)]} \quad (19)$$

where γ_r is the ratio of shear strains in the discrete columns relative to the surrounding soil in terms of shear-strain ratio. Based on three-dimensional finite element numerical analysis results, Rayamajhi et al. [21] found that the γ_r predominantly depends upon the G_r and is only slightly affected by other parameters such as A_r or the column-length-to-diameter ratio (L/D) (for values of 4.5–30).

$$\gamma_r = 1.04(G_r)^{-0.65} - 0.04 \leq 1.0 \quad (20)$$

4.3. Correction for soil behavior type index for post-grouting

In CPT data interpretation, I_c is a very important index that is used widely to identify soil type, to correlate fines contents as well as other soil parameters. For example, when $I_c \geq 2.6$, the soil type is identified as clay-like soil and when $I_c < 2.6$, the soil type is identified as sand-like soil [14].

When utilizing CPT to verify the effectiveness of ground improvement, a phenomenon arises, wherein the I_c calculated based on post-grout CPT data decreases compared to that calculated based on pre-grout CPT data. Fig. 7 shows the comparison of I_c of pre-grout CPT-01 and I_c of post-grout CPT-01A. The average decrease of I_c between pre- and post-grout is 0.15, while the decrease between depths of 3.2 and 5.4 meters is 0.32. When I_c is used to identify soil type, this decrease results in an apparent soil type change, in this example, from silty soil to sandy soil. However, common sense dictates that the column-type ground improvement did not actually change the soil type. Therefore, this apparent soil type change is misleading. The author called this phenomenon the "*pseudo-sandification phenomenon.*"

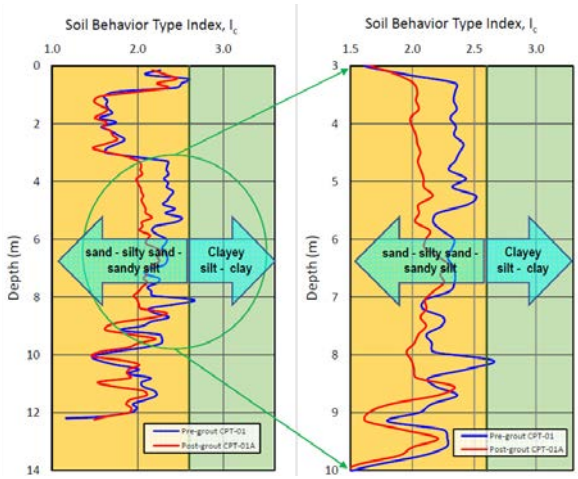

Figure 7. Changes of Soil Behavior Type Index, I_c, Due to Grouting

Because I_c is used to calculate fines contents and further to calculate the eqivalent clean sand normalized CPT penetration resistance, q_{c1Ncs} [2] or $Q_{tn,cs}$ [14], this *pseudo-sandification phenomenon* might well under-estimate q_{c1Ncs} or $Q_{tn,cs}$ and further over-estimate the liquefaction potential and liquefaction-induced settlement, resulting in an under-estimation of the ground improvement performance itself. In order to avoid this kind of under-estimation, the post-grout I_c should not be directly utilized. A correction to post-grout I_c is necessary. If the pre-grout CPT data can represent the soil profile at the post-grout CPT location (for example, the distance between the two CPTs is small), the preferable correction is to directly replace the post-grout SBT Index with pre-grout SBT index, that is, using $(I_c)_{post} = (I_c)_{pre}$. If it is not the case, at a minimum, a constant increment should be added to the calculated post-grout I_c, so that $(I_c)_{post,used} = (I_c)_{post,calculated} + \Delta I_c$.

4.4. Correction for fines contents

As noted in Section 2.2, the soil profile at this project site consists predominantly of silty sand layers with relatively high fines content (FC). The fines contents are between 42% and 46% at depths above 7.6 meters and between 35% and 49% at depths below 12.2 meters. Lew and Tran [25] reported a case history of a site in the western San Fernando Valley where the alluvial deposits were predominantly sandy silt or silty sand with FC by weight between about 47% and 70%. Evidence of liquefaction-induced settlement was observed a few days after the January 17, 1994, Northridge earthquake by Lew. Lew [25] found that "the observed settlement of the ground surface is substantially smaller than the settlement predicted by currently used methods for estimating settlement for clean sands."

Little literature is available related to liquefaction-induced settlement for soils with FC higher than 35%. In the investigation of the seismic compression characteristics of unsaturated nonplastic and low-plasticity silty sands with varying FC, the UCLA research group Yee et al. [26] and Steward [27]) found that increasing FC generally decreases the volume change for fines fractions consisting of silts and clayey silts of moderate-to-low plasticity ($PI \leq 10$). They found that

$$(\varepsilon_v)_{FC} = K_{FC} \cdot (\varepsilon_v)_{FC=0} \quad (21)$$

and

$$\begin{aligned} K_{FC} &= 1 && (FC = 0 - 10\%) \\ K_{FC} &= e^{[-0.042(FC-10)]} && (FC = 10\% - FC_L) \\ K_{FC} &= 0.35 && (FC \geq FC_L) \end{aligned} \quad (22)$$

where $(\varepsilon_v)_{FC}$ is the volumetric strain with any FC value and $(\varepsilon_v)_{FC=0}$ is the volumetric strain at $FC = 0$, i.e., the volumetric strain of clean sand. The limiting fines content FC_L is ~35% for most of the materials considered in their study.

Yee et al. [26] also investigated the effect of saturation (S) on seismic compression volumetric strain and found that

$$(\varepsilon_v)_{S\geq 60\%} = (\varepsilon_v)_{S=0\%} \quad (23)$$

Although further verification studies are needed, it is the opinion of the authors that Eq. (22) and Eq. (23) should also be applicable to any liquefaction-induced volume change calculations, i.e.,

$$\left[(\varepsilon_v)_{liq}\right]_{FC} = K_{FC} \cdot \left[(\varepsilon_v)_{liq}\right]_{FC=0} \quad (24)$$

5. Post-grout seismic settlement

5.1. Comparison of predicted settlement

Fig. 8 shows a comparison of the calculated liquefaction-induced settlement (S_{liq}) using the data from Grid A (SPT-1, pre-grout CPT-1, and post-grout CPT-1A). For comparison, the pre-grout SPT results are also included. It can be seen that the predicted pre-grout S_{liq} agrees very well with both SPT and CPT data, using both the traditional FC correction and with the Eq. (22) FC correction.

For post-grout CPT data, the calculated S_{liq} is only reduced by 37% using traditional FC corrections even

though the tip resistance below a depth of 3 meters increased by an average of 240% and the friction increased by an average of 350% post grouting (both comparisons exclude extreme high values obtained). Considering the shear stress reduction effects caused by CG columns, the reduction is only slightly increased, from 37% to 40%. This slight increase of reduction demonstrates that the shear stress reduction caused by the GC column effect is not significant. When corrected for I_c, the S_{liq} is reduced by 60% for a constant I_c increament correction, i.e., $((I_c)_{post,used} = (I_c)_{post,calculated} + \Delta I_c.)$, and by 65% when using pre-grout SBT Index correction, i.e., $(I_c)_{post} = (I_c)_{pre}$.

These results demonstrate that in the evaluation of post-grout behavior using CPT data, the post-grout I_c correction is very important. The preferable method of correction is to directly use the pre-grout $(I_c)_{pre}$. The results also demonstrate that if suitable pre-grout CPT data is not available, for example, from a nearby location, the I_c correction using a constant increment ΔI_c should also give a reasonable estimation of settlement.

When incorporating the FC correction using Eq. (22), the S_{liq} is reduced by 76% from 26.9 centimeters to 6.4 centimeters by the Boulanger and Idriss's method [3, 4]. This value seems reasonable considering the increases in post-grout CPT tip resistance and friction.

For comparison, the S_{liq} calculated using Robertson's method [14] is also shown in Fig. 8. Generally, Robertson's method yields a smaller S_{liq} value when compared to the Boulanger and Idriss's method.

Fig. 9 shows an example of the graphical output of liquefaction potential and the induced settlement of post-grout CPT-01A.

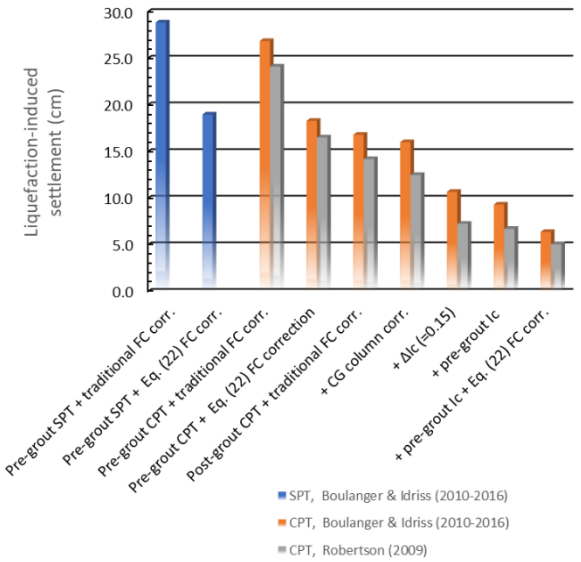

Figure 8. Comparison of Liquefaction-Induced Settlements with Various Affecting Factors

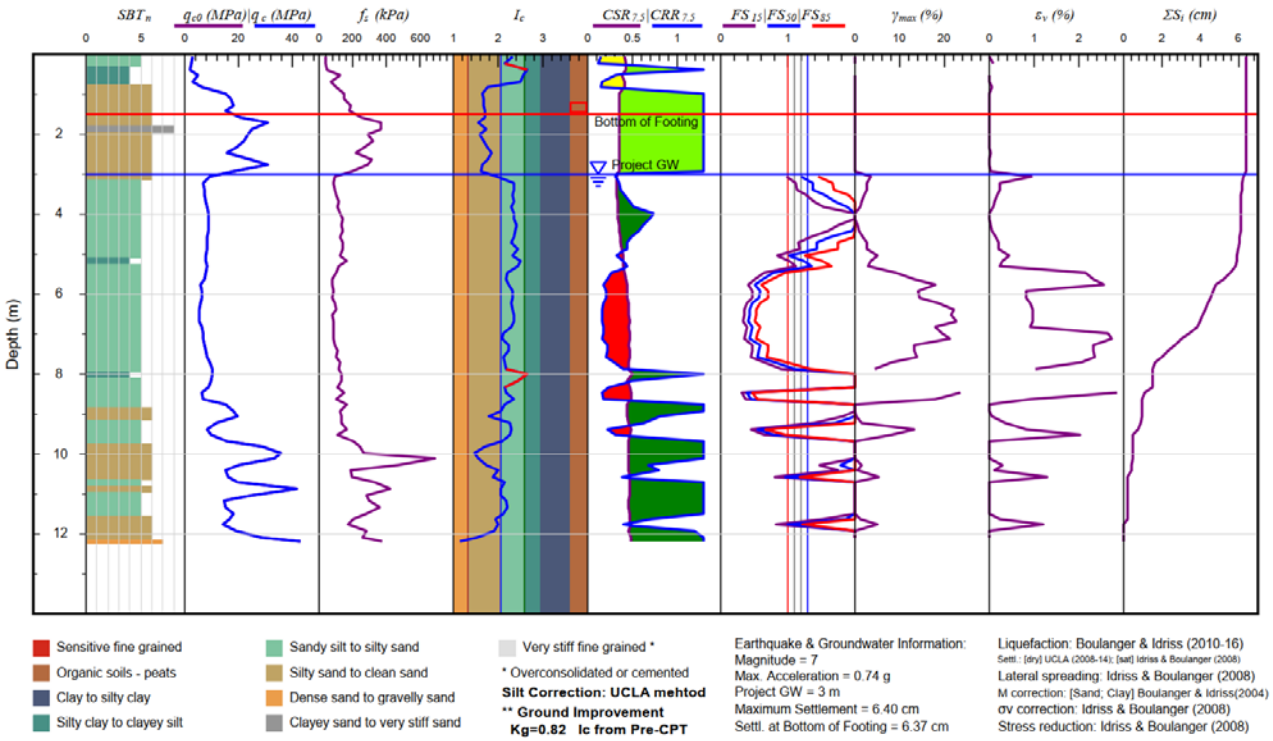

Figure 9. Example of Liquefaction and Seismic Settlement Calculations of Post-Grout CPT-1A

5.2. Modification of CG program

Fig. 8 indicates that after applying all corrections, the post-grout liquefaction-induced settlement is estimated to be 6.4 centimeters using the Boulanger & Idriss method [2, 4] and 5.1 cm using Robertson's method [14]. As mentioned in Section 3, the design allowable settlement is 2.5 centimeters for this project. The estimated post-grout settlement is greater than the allowable value for the original proposed ground improvement program. As shown in Fig. 9, local partial liquefaction is still anticipated. For this reason, a discussion was held among the project team members. As a result of this discussion, a modified CG program was

proposed. The modified CG program included adding another CG point in the center of the original CG grid. Additional post-grout CPTs were performed after grouting of the additional points. The modified CG program is illustrated in Fig. 10. Two test grids (Grid A and Grid C) were utilized. Grid A is an addition to the original Grid A. Grid C is a new test area. Five post-grout CPTs were performed at Grid A and six post-grout CPTs were performed at Grid C.

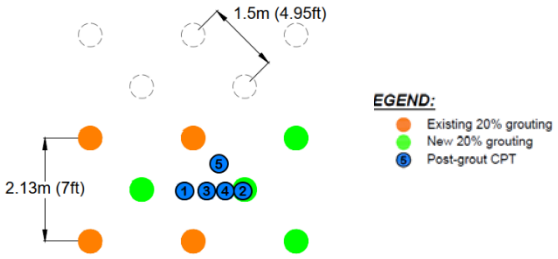

Figure 10. Modification of CG Program

Fig. 11 shows the profiles of CPT tip resistance (q_c) and friction (f_s) of Grid A. For comparison, pre-CPT profiles and post-CPT profiles from the original $2.1m \times 2.1m$ grid CG are also shown in Fig. 11. It can be seen that with the added CG point in the $2.1m \times 2.1m$ grid (becoming a $1.5m \times 1.5m$ grid), the increase to q_c and f_s is significant. Fig. 11 illustrates only the post-CPT-01 and post-CPT-05 profiles for the $1.5m \times 1.5m$ modified grid. Post-CPT-02, -03 and -04 were performed in order to observe the variation in CPT resistance with the distance to the center of the CG point. However, these CPTs were not illustrated in Fig. 11 because shallow refusals were encountered.

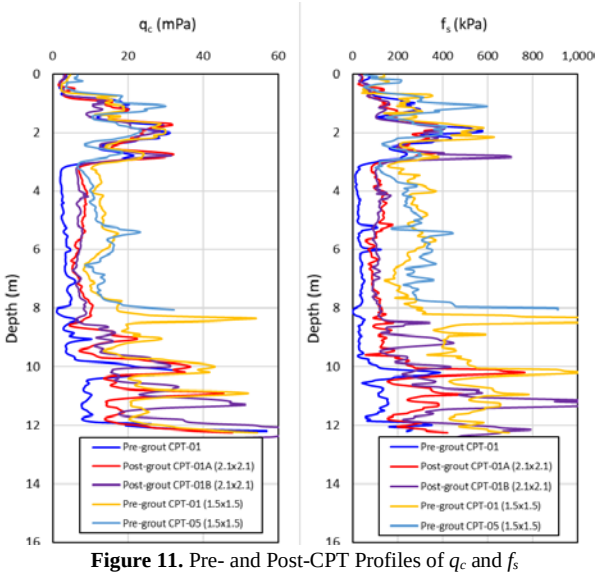

Figure 11. Pre- and Post-CPT Profiles of q_c and f_s

Similar results were obtained from Grid C.

With the additional CG point, the calculated S_{liq} values are all reduced to less than 1 centimeter, which satisfies the project's allowable settlement criteria.

6. Conclusions and discussions

Compaction grouting was proposed for a project site as the ground improvement method to mitigate the liquefaction hazard. A test program was performed in order to verify the effectiveness of the CG method before commencing grouting of the entire site. The test program consisted of performing test grouting in two test grids and performing CPT soundings before and after test grouting. Evaluating procedures and the factors affecting the evaluation of CG performance were discussed. Based on the examination of the test program results, the following conclusions can be reached.

1. Compaction grout (CG) can be used to densify soils with high fines content and mitigate liquefaction potential. However, in order to improve the effectiveness of CG, a well designed and executed test program is important.
2. When utilizing CPT to verify the effectiveness of column-type ground improvement, the post-grout CPT data must account for the apparent modification of the soils thus treated in order to yield accurate results. The modification phenomenon observed and demonstrated in this paper is termed "*pseudo-sandification phenomenon*" by the authors. In order to yield accurate post-grout results, this phenomenon has to be accounted for. The preferable method of correction of this phenomenon is to directly replace the post-grout SBT Index with pre-grout SBT index, that is, using $(I_c)_{post} = (I_c)_{pre}$. The actual post-grout liquefaction-induced settlement is very sensitive to this correction.
3. If suitable pre-grout CPT data is not available, for example, from an appropriate area nearby, a correction using a constant increment ΔI_c, i.e., $(I_c)_{post,used} = (I_c)_{post,calculated} + \Delta I_c$, can also be substituted to provide a reasonable estimation of the pre-grout conditions.
4. For soils with FC higher than 35%, the correction of the liquefaction-induced volumetric strain for fines contents is important. Although further verification studies are needed, it is the authors' opinion that the FC correction to volumetric strain proposed by Yee et al. [26] would be applicable.
5. Although it should be considered, the shear stress reduction correction for column-type improvement is not as important as the I_c and FC corrections.
6. For the same replacement ratio, more dense grout grids provide better improvement. An optimum grid size is important and should be determined by a test program.

Based on the results of this study, the authors believe that further research and improvements for the following topics are needed.

1. In order to reasonably evaluate the effectiveness of ground improvement, the involvement of an experienced geotechnical engineer from the beginning of the planning stage is very important.
2. In the current study, because of the limitation of the simplified liquefaction evaluation procedures,

only the post-grout behavior of the soils the CG columns was examined. The contribution of CG column itself was excluded. A total evaluation of the post-grout behavior of the densified soils and the CG columns is necessary. In order to develop a method that can appropriately evaluate the total post-grout behavior and can be applied in the practice, centrifuge model tests or three-dimensional finite element method studies are necessary.

3. Further verification studies for the application of the FC correction proposed by Yee et al. [26] are needed.

References

[1] Morton, D. M., and Miller, F. K. (2006). "Geologic Map of the San Bernardino and Santa Ana 30 minute by 60 minute Quadrangles, California." U.S. Geological Survey Open-File Report 2006-1217, Scale: 1:100,000.

[2] Idriss, I. M., and Boulanger, R. W. (2008). "Soil Liquefaction During Earthquake." Earthquake Engineering Research Institute, EERI Publication MNO-12.

[3] Boulanger, R. W., and Idriss, I. M. (2014). "CPT and SPT based liquefaction triggering procedures." Rep. No. UCD/CGM-14/01, Univ. of California, Davis, CA.

[4] Boulanger, R. W., and Idriss, I. M. (2015). "CPT-based liquefaction triggering procedure." Journal of Geotechnical and Geoenvironmental Engineering, ASCE, 04015065, 10.1061/(ASCE)GT.1943-5606.0001388.

[5] Youd, T. L., and Idriss, I. M. (2001). "Liquefaction Resistance of Soil: Summary Report from the 1996 NCEER and 1998 NCEER/NSF Workshops on Evaluation of Liquefaction Resistance of Soils." Journal of Geotechnical and Geoenvironmental Engineering, Vol. 127, No. 4, April 2001, pp. 297-313.

[6] Idriss, I. M., and Boulanger, R. W. (2004). "Semi-empirical procedures for evaluating liquefaction potential during earthquakes." Proc., 11th Int. Conference on Soil Dynamics and Earthquake Engineering, and 3rd Int. Conference on Earthquake Geotechnical Engineering, D. Doolin et al., eds., Stallion Press, Vol. 1, 32-56.

[7] Yi, F. (2019). "GeoSuite©, version 2.4 - A Comprehensive Package for Geotechnical and Civil Engineers." http://geoadvanced.com/

[8] Seed, H. B., and Idriss, I. M. (1971). "Simplified procedure for evaluating soil liquefaction potential." J. Soil Mechanics and Foundations Div., ASCE97(SM9), 1249-273.

[9] Seed, H. B., and Idriss, I. M. (1982). "Ground motions and soil liquefaction during earthquakes." Earthquake Engineering Research Institute, Monograph Series, Monograph No. 5.

[10] Seed, H. B., and Tokimatsu, K., Harder, L. F., and Chung, R. M. (1985). "The influence of SPT procedures in soil liquefaction resistance evaluations." J. Geotech. Engrg., ASCE, 111(12), 1425-1445.

[11] Liao, S. C., and Whitman, R. V. (1986). "Overburden correction factors for SPT in sand." J. Geotech. Engrg., ASCE, 1986, 112(3), 373-377.

[12] Idriss, I. M. (1999). "An update to the Seed-Idriss simplified procedure for evaluating liquefaction potential." in Proceedings, TRB Workshop on New Approaches to Liquefaction, Publication No. FHWA-RD-99-165, Federal Highway Administration, January.

[13] Robertson, P. K. and Wride, C. E. (1998) "Evaluating cyclic liquefaction potential using the cone penetration test." Canadian Geotechnical Journal, 35: 442-459.

[14] Robertson, P. K. (2009). "Performance based earthquake design using the CPT", Proceedings of The International Conference on Performance-Based Design in Earthquake Geotechnical Engineering (IS-Tokyo 2009), 15 -18 June 2009.

[15] Robertson, P. K. (2009). "Interpretation of Cone Penetration Tests - a unified approach", Canadian Geotechnical Journal, 2009, 46(11): 1337-1355.

[16] Zhang, G., Robertson, P. K., and Brachman, R. W. I. (2002). "Estimating liquefaction-induced ground settlements from CPT for level ground" Canadian Geotechnical Journal, Ottawa, 39: 1168-1180.

[17] Ishihara, K., and Yoshimine, M. (1992). "Evaluation of settlements in sand deposits following liquefaction during earthquakes." Soils and Foundations 32(1), 173-188.

[18] Yoshimine, M., Nishizaki, H., Amano, K., and Hosono, Y. (2006). "Flow deformation of liquefied sand under constant shear load and its application to analysis of flow slide in infinite slope." Soil Dynamics and Earthquake Eng. 26, 253-264.

[19] Baez, J. I., and Martin, G. R. (1993). "Advances in the design of vibro systems for the improvement of liquefaction resistance." Proc., 7th Annual Symp. of Ground Improvement, Canadian Geotechnical Society, Vancouver, BC, Canada.

[20] Baez, J. I. (1995). "A design model for the reduction of soil liquefaction by using vibro-stone columns." Ph.D. thesis, Univ. of Southern California, Los Angeles.

[21] Rayamajhi, D., et al. (2014). "Numerical study of shear stress distribution for discrete columns in liquefiable soils." J. Geotech. Geoenviron. Eng., 2014, 140(3): 04013034.

[22] Rayamajhi, D., et al., (2015). "Dynamic centrifuge tests to evaluate reinforcing mechanisms of soil-cement columns in liquefiable sand." J. Geotech. Geoenviron. Eng., 2015, 141(6): 04015015.

[23] Rayamajhi, D., Ashford, S. A., Boulanger, R. W., and Elgamal, A. (2016). "Dense granular columns in liquefiable soils: Shear reinforcement and cyclic stress ratio reductions." J. Geotech. Geoenviron. Engrg., 2016, 142(7): 04016023.

[24] Rayamajhi, D., Boulanger, R. W., Ashford, S. A., and Elgamal, A. (2016). "Dense granular columns in liquefiable ground: Effects on deformations." J. Geotech. Geoenviron. Engrg., 2016, 142(7): 04016024.

[25] Lew, M., and Tran, L. (2012). "Case History of Observed Liquefaction-Induced Settlement Versus Predicted Settlement." Proceedings of The Fifteenth World Conference on Earthquake Engineering, Lisbon, Portugal, 2012.

[26] Yee, E., Duku, P. M., and Stewart, J. P. (2014). "Cyclic volumetric strain behavior of sands with fines of low plasticity." J. Geotech. Geoenviron. Engrg., ASCE, 140(4), 04013042 (10 pages).

[27] Stewart, J. P. (2014). Notes on Seismic Compression of Compacted Soils, C&EE 225 - Geotechnical Earthquake Engineering, University of California, Los Angeles.